SWOSU Journal of Undergraduate Research

Volume 1 Article 2

11-1-2014

Transition Metal Complexes of Dibenzyl Tetraazamacrocycles

Ashlie N. Walker

Megan A. Ayala

Mackenzie C. Bergagnini

P. John D. Bui

Stephanie N. Chidester

See next page for additional authors

Transition Metal Complexes of Dibenzyl Tetraazamacrocycles

Authors

Ashlie N. Walker, Megan A. Ayala, Mackenzie C. Bergagnini, P. John D. Bui, Stephanie N. Chidester, Chad I. Doeden, Louise Sweany, and Tim Hubin

Transition Metal Complexes of Dibenzyl Tetraazamacrocycles

by Ashlie N. Walker, Megan A. Ayala, Mackenzie C. Bergagnini, P. John D. Bui, Stephanie N. Chidester, Chad I. Doeden, Louise Esjornson, Brian R. Sweany
(Prof. Tim Hubin, Department of Chemistry)

Tetraazamacrocycles, cyclic molecules with four nitrogen atoms, have long been known to produce highly stable transition metal complexes. Cross-bridging such molecules with 2-carbon chains has been shown to enhance the stability of these complexes even further, providing enough stability to use the resulting compounds in applications as diverse and demanding as aqueous, green oxidation catalysis all the way to drug molecules injected into humans. Although the stability of these compounds is believed to result from the increased rigidity and topological complexity imparted by the cross-bridge, there is insufficient experimental data to exclude other causes. In this study, standard organic and inorganic synthetic methods were used to produce unbridged dibenzyl tetraazamacrocycle analogues of known cross-bridged tetraazamacrocycles and their transition metal complexes to allow direct comparison of molecules identical except for the cross-bridge. The syntheses of the known tetraazamacrocycles and the novel transition metal complexes were successful with high yields and purity. Initial chemical characterization of the complexes by UV-Visible spectroscopy and cyclic voltammetry shows little difference in electronic properties from bridged versions. Direct comparison studies of the unbridged and bridged compounds' stabilities remain to be carried out and will shed light on the importance of the cross-bridge to complex robustness.

Introduction

Ligands are organic molecules containing atoms, like nitrogen, which have lone pairs of electrons capable of interacting with metal ions to form *complexes* where the ligand and the metal ion combine

to form a new compound with distinct and often useful new properties. *Tetraazamacrocycles* are common ligands containing four nitrogen atoms tied together in a ring by carbon chains. The stability of transition metal complexes can be characterized by their kinetic stability (how long it takes to decompose the complex under harsh conditions) and/or their thermodynamic stability (energy values which can be determined for any molecule; lower energy equals more stability). Inorganic chemists have learned that the kinetic stability of metal complexes can be increased by many orders of magnitude by increasing the *topological complexity* (number of links between the nitrogen atoms) and rigidity of the ligand. In general, complex kinetic stability decreases in the series bridged azamacrocycle ligand > azamacrocyclic ligand > linear ligand with more than one nitrogen > single nitrogen ligand.[1]

Cross-bridged tetraazamacrocycles having an additional 2-carbon bridge between non-adjacent nitrogen atoms of a tetraazamacrocycle, which are particularly rigid and lead to very kinetically stable metal complexes, have been extensively studied by Hubin, *et. al.*[2] This stability confers on these transition metal complexes great promise in such applications as homogeneous catalysis, where complex stability has historically been a problem. However, specific studies where "control" metal complexes, identical in all ways except lacking the ligand cross-bridge, have not been prepared and characterized with respect to complex stability, as well as other properties. For cross-bridged complexes, there is a need to probe the thermodynamic stability at the same time as the kinetic stability, to make sure that the increase in the latter is not a byproduct of change in the former, but rather due to topological and rigidity factors alone.

Electronic properties (specifically of the metal d-electrons) of tetraazamacrocycle transition metal complexes are influenced by their geometric structure and the pattern of the nitrogen atom substituents.[3] If these properties are very similar between bridged and unbridged complexes of the same metal ion, that indicates that the bridge has little effect on the d-electron configuration. The d-electron configuration would be most closely associated with

thermodynamic stability, which would therefore be assumed to be approximately the same for the bridge/unbridged pair. However, if the kinetic stability of the bridged complex is much greater than its unbridged analogue, then these results would be consistent with the hypothesis that the topological complexity and additional rigidity of the cross-bridge is responsible for the additional kinetic

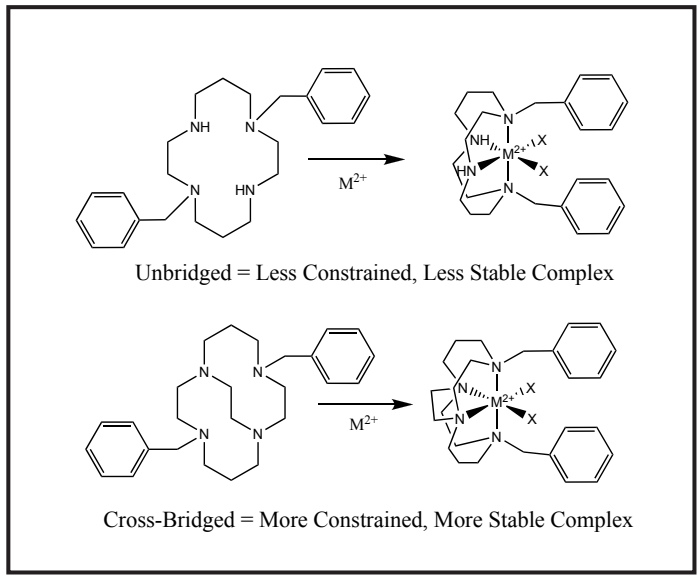

Figure 1. Unbridged vs. Cross-bridged tetraazamacrocycles and complexes

stability of cross-bridged complexes, not any thermodynamic stabilization.

We report here modified methods[4] for synthesizing known dibenzyl cyclen and cyclam (common names based on the ring size) tetraazamacrocycle ligands 1,7-dibenzylcyclen (**1**) and 1,8-dibenzylcyclam (**2**) (numbers indicate the location on the ring of the benzyl groups) and their transition metal complexes. The cyclam ligand has been complexed to a number of metal ions previously,[5] but the characterization of its complexes has been limited. The cyclen analogue has no published complexes. Therefore, we aimed to synthesized and characterize the complexes

of these two analogous tetraazamacrocycle ligands for comparison. In particular, we wanted to contrast the properties of these unbridged complexes with the known cross-bridged complexes.

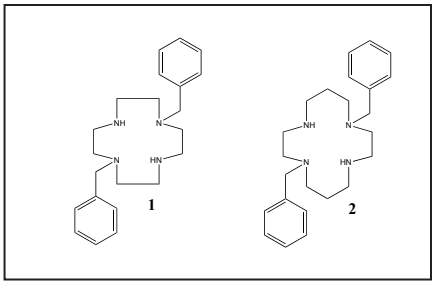

Figure 2. 1,7-dibenzylcyclen (1) and 1,8-dibenzylcyclam (2)

Materials and Methods

General

N,N'-bis(amino-propyl) ethyl-enediamine (98%) was purchased from Acros Organics. Glyoxal (40% wt in water), methyl iodide (99%), and sodium borohydride (98%) were purchased from Aldrich Chemical Co. Cyclen was purchased from Strem Chemical Co. All solvents were of reagent grade and were dried, when necessary, by accepted procedures.[6] Cyclam was prepared according to a modified literature method from N,N'-bis(aminopropyl)ethylenediamine.[7] Elemental analyses were performed by Quantitative Technologies Inc. Electrospray Mass spectra were collected on a Shimadzu LCMS-2020 instrument. NMR spectra were obtained on a Varian Bruker AVANCE II 300 MHz NMR Spectrometer instrument. IR spectra of the samples as KBr pellets were recorded on a Thermo-Nicolet 380 FTIR Spectrometer. Electronic spectra were recorded using a Beckman Coulter DU800 UV-Vis Spectrometer. Conductance measurements were obtained with an Oakton CON510 Bench Conductivity/TDS Meter on 0.001 M solutions at room temperature. Magnetic moments were obtained on finely ground solid samples at ambient temperatures using a Johnson Matthey MSB Auto magnetic susceptibility balance. Electrochemical experiments were performed on a BAS Epsilon EC-USB Electrochemical Analyzer. A button Pt electrode was used as the working electrode with a Pt-wire counter electrode and a Ag-wire pseudo-reference electrode. Scans were taken at 200 mV/s. Acetonitrile solutions of the complexes (1 mM) with tetrabutylammonium hexafluorophosphate (0.1 M) as a supporting electrolyte were used. The measured potentials were referenced to SHE using ferrocene (+0.400 V versus SHE) as an

internal standard. All electrochemical measurements were carried out under N_2.

Tetracyclen (4): 26.3 g (0.153 mol) of cyclen (**3**) and 105 ml of acetonitrile were added to a 500 ml roundbottom flask, which was then flushed for 15 minutes with N_2 gas. 22 ml (8.88 g or 0.153 mol) of 40 % by mass glyoxal solution was added and the reaction stirred under N_2 at 50-65 °C for 2 hours. The solvent was removed and the brown residue was extracted with 5 x 50 ml portions of chloroform. Following filtration, the chloroform solution was

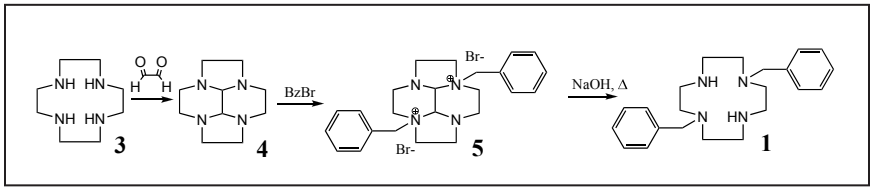

Figure 3. Synthetic scheme for 1,7-dibenzylcyclen (1)

evaporated to give the product as an oil. The product was purified by column chromatography using neutral Brockman I alumina with 1% MeOH in CH_2Cl_2 as the eluent. Yield = 22.327 g (75%). Electrospray mass spec: m/z at 195 = LH^+.

Dibenzyltetracyclen (5): 10.53 g (0.0543 mol) of **4** was dissolved in 300 ml dry acetonitrile and added to a 500 ml roundbottom flask. 97 ml (0.8145 mol, 15 eq) of benzyl bromide was added, the flask stoppered, and then stirred at room temperature for 4 days. [CAUTION: benzyl bromide is an extreme lachrymator; use only in a chemical fume hood.] The white solid product was filtered on a fine glass frit, washed with acetonitrile and then ethyl acetate to remove excess benzyl bromide. The solid was vacuum dried to give 25.7 g of pure product (88% yield). Electrospray mass spec: m/z = 455 $(L - Br)^+$. Elemental analysis calc for $C_{24}H_{32}N_4Br_2$: C 53.73, H 5.97, N 10.45; found C 53.52, H 6.00, N 10.30.

1,7-dibenzylcyclen (1): 36.115 g (0.0673 mol) of **5** and 360 ml of 3 M aqueous NaOH were added to a 500 ml roundbottom flask. The flask was stirred and heated in an oil bath at 80 °C for 3 days under nitrogen. A yellow solution with an orange oil floating on top resulted, and was cooled and extracted with 5 portions of

80 ml of CH_2Cl_2. The organic layers were combined, dried over $MgSO_4$, filtered, and evaporated to give an orange foamy solid product (20.656 g, 87% yield). Electrospray mass spectrum: m/z = 353 (LH^+). Elemental analysis calculated for $C_{22}H_{32}N_4 \cdot 3H_2O$: C 64.99, H 9.42, N 13.78; found C 65.61, H 8.61, N 13.45.

BMBcyclam (7): 12.0 g (0.060 mol) of cyclam (**6**) was added to a 2 L roundbottom flask and stirred with 600 ml of CH2Cl2 and 600ml of 30% NaOH. This solution was then refluxed under a N2 atmosphere for 36 hours. The biphasic solution was extracted four times with 100 ml CH_2Cl_2. The combined organic layer was dried over $MgSO_4$ for one hour, then filtered, evaporated, and dried under vacuum to obtain 7. Yield = 12.25 g (91%). Electrospray

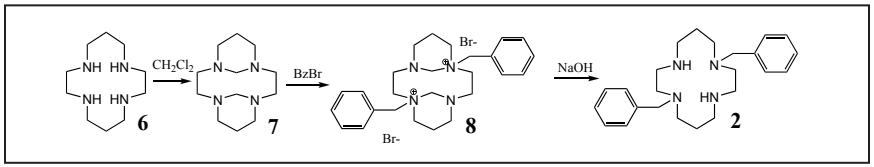

Figure 4. Synthetic scheme for 1,8-dibenzylcyclen (2)

mass spectrum: m/z = 225 (LH^+). NMR (^1H and ^{13}C) gave peak regions of 2.17-3.10 ppm for macrocycle hydrogens, and peaks at 19.4, 48.4, and 68.0ppm for unique carbons.

DibenzylBMBcyclam (**8**): 12.0 g of **7** was dissolved in 250 ml of acetonitrile in a 500 ml roundbottom flask. 3 equivalents of benzyl bromide was added and stoppered. This solution was stirred for a week at room temperature. The white solid produced was collected on a glass frit, washed with 50 ml of ethyl acetate to ensure all benzyl bromide was removed, and then dried under vacuum. Yield = 27.3 g (90%) Electrospray mass spectrum: m/z = 203 m/z $(L\text{-}2Br)^{2+}$, m/z = 407 $(L\text{-}2Br)^+$, and m/z = 487 $(L\text{-}Br)^+$. NMR gave peak regions for macrocycle hydrogens at 1.76-3.60ppm, benzyl hydrogens 4.31-4.65ppm. Unique carbons were seen at 19.4, 47.6, 51.3, 59.6, 62.9, 76.8 ppm.

1,8-dibenzylcyclam (2): 22.0 g of **8** was dissolved in 500 ml of 3 M NaOH in a 1 liter Erlenmeyer flask. This solution was stirred for 3 hours at room temperature. The solution was then

extracted with five times 150 ml of $CHCl_3$. All organic layers were collected and dried over $MgSO_4$, then filtered. The solution was evaporated and dried under vacuum to obtain **2**. Yield = 13.6 g (92%). Electrospray mass spec: m/z = 381 (LH). NMR (^1H and ^{13}C) analysis gave peak regions of, 1.85, and 2.51-2.74, 3.71 ppm for macrocycle hydrogens and 4.72ppm for benzyl hydrogens. Six unique carbon peaks were found at 26.0, 47.7, 50.2, 52.0, 54.2, and 58.2ppm.

Metal complexation: All complexation reactions were performed in an inert atmosphere glovebox. All complexations used one equivalent of anhydrous metal acetate ($M(C_2H_3O_2)_2$) salts in anhydrous methanol (20 ml) reacted with one equivalent of macrocyclic ligand. Complexations of **1** used 0.705g (0.0020mol)

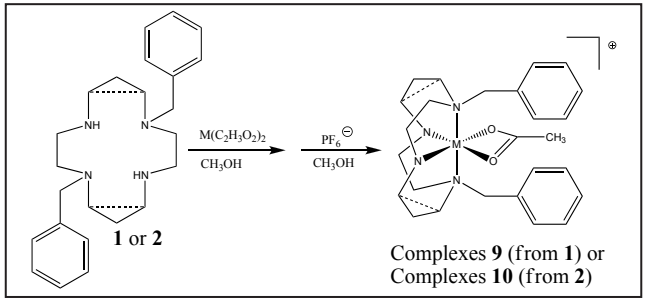

Figure 5. Metal complexation reactions

of ligand **1**; complexations of **2** used 0.425g (0.0011mol) of ligand **2**. The following specific example is typical of all eight complexation reactions.

0.425 g (0.0011 mol) of 1,8-dibenzylcyclam and 0.195 g (0.0011 mol) of anhydrous cobalt(II) acetate were added to a 20 ml reaction vial and 15 ml of anhydrous methanol was added. The reaction was stirred at room temperature for 7 days. The reaction vial was removed from the glovebox and the workup was done in air. The reaction solution was filtered through celite in a Pasteur pipette into a 100 mL roundbottom flask to remove any trace solids. Separately, 5 equivalents (0.0055 mol, 0.897 g) of NH_4PF_6 was dissolved in a minimal amount of methanol (~5 ml). This solution was filtered through a chemwipe in a pipette and into the stirring

metal complex solution. Precipitate of the pink complex as a PF_{6-} salt formed immediately. The reaction flask was placed in a freezer (-10 °C) for 1 hour to complete the precipitation of the product. The solid pink powder product was collected on a fine glass frit, washed with a minimal amount of cold methanol, then ether. The product was transferred to a 4-dram vial and dried overnight under vacuum. Yield = 0.506 g (70%).

[Note: one exception to the procedure above was required for the $[Ni(Bn_2Cyclen)(OAc)]PF_6$ complex. It did not precipitate from methanol. Therefore, it was evaporated to dryness and ~50 ml of water was added. The pale blue product was not water soluble and was filtered from the water solution.]

Results and Discussion

Complex Synthesis

Both ligands are known in the literature and our syntheses of them yielded pure compounds in good yield (57% yield for three steps for **1**; 75% yield for three steps for **2**). Complexation occurred as expected in methanol for both ligands with all four divalent metal ions (Co, Ni, Cu, and Zn) from their acetate salts. Macrocycle complexes with acetate counter anions are typically hygroscopic oils, so we did not try to isolate them. Instead we performed an anion metathesis reaction with hexafluorophosphate to give the $[M(ligand)(acetate)]PF_6$ complexes, which precipitate out of methanol and are non-hygroscopic powders. Formulas, yields, electrospray mass spec peaks, and elemental analysis data for all eight complexes are given in **Table 1** and **Table 2** below.

All of the complexes were formed, based on the expected color changes and dissolution of the ligand and metal salt during the reactions. Additional evidence of complexation is shown by the multiple peaks in the electrospray mass spectrum for each complex containing both the metal and the ligand and sometimes other species as well (acetate, hexafluorophosphate, water, see **Table 1**). Yields were typically from 50%-75%, which are acceptable. These yields were likely lowered for several of the complexes by considerable solubility in the methanol solution they

Table 1. Yields and selected peaks in the electrospray mass spectra of ligand **1** and **2** complexes

Expected Complex	Color	Yield (g)	Yield(%)	m/z	m/z
[Co(**1**)(OAc)]PF_6 (**9a**)	pink-purple	0.506	71%	499 $Co(\mathbf{1})(OAc)^+$	439 $Co(\mathbf{1})^+$
[Ni(**1**)(OAc)]PF_6 (**9b**)	pale sky blue	0.324	46%	498 $Ni(\mathbf{1})(OAc)^+$	219 $Ni(\mathbf{1})^{2+}$
[Cu(**1**)]$(PF_6)_2$ (**9c**)	bright blue	0.291	37%	524 $Cu(\mathbf{1})(OAc)(H_2O)^+$	222 $Cu(\mathbf{1})^{2+}$
[Zn(**1**)(OAc)]PF_6 (**9d**)	light tan	0.400	56%	505 $Zn(\mathbf{1})(OAc)^+$	464 $Zn(\mathbf{1})(H_2O)^+$
[Co(**2**)(OAc)]PF_6 (**10a**)	pale pink	0.680	54%	470 $Co(\mathbf{2})(OAc)^+$	410 $Co(\mathbf{2})^+$
[Ni(**2**)(OAc)]PF_6 (**10b**)	pale sky blue	0.927	75%	469 $Ni(\mathbf{2})(OAc)^+$	205 $Ni(\mathbf{2})^{2+}$
[Cu(**2**)]$(PF_6)_2$ (**10c**)	brick red	1.055	72%	560 $Cu(\mathbf{2})(PF_6)^+$	208 $Cu(\mathbf{2})^{2+}$
[Zn(**2**)(OAc)]PF_6 (**10d**)	off-white	0.945	76%	475 $Zn(\mathbf{2})(OAc)^+$	436 $Zn(\mathbf{2})(H_2O)^+$

Table 2. Formulas and elemental analyses of ligand **1** and **2** complexes

Complex Formulation for Elemental Analysis	Calc C	Calc H	Calc N	Found C	Found H	Found N
(**9a**) $[Co(C_{24}H_{36}N_4)(C_2H_3O_2)]PF_6 \cdot 1.0\ H_2O$	47.21	6.25	8.47	47.45	6.07	8.53
(**9b**) $[Ni(C_{24}H_{36}N_4)(C_2H_3O_2)]PF_6 \cdot 1.0\ H_2O$	47.22	6.25	8.45	47.54	6.25	8.29
(**9c**) $[Cu(C_{24}H_{36}N_4)](PF_6)_2 \cdot 1.0\ H_2O$	38.33	5.09	7.45	38.69	4.74	7.38
(**9d**) $[Zn(C_{24}H_{36}N_4)(C_2H_3O_2)]PF_6 \cdot 0.1\ H_2O$	47.91	6.06	8.60	47.62	5.82	8.44
(**10a**) $[Co(C_{22}H_{32}N_4)(C_2H_3O_2)]PF_6$	45.50	5.89	8.84	45.12	5.52	8.65
(**10b**) $[Ni(C_{22}H_{32}N_4)(C_2H_3O_2)]PF_6 \cdot 1.0\ H_2O$	45.52	5.89	8.85	45.66	5.07	8.65
(**10c**) $[Cu(C_{22}H_{32}N_4)](PF_6)_2 \cdot 1.0\ NH_3$	36.55	4.88	9.69	38.60	5.01	9.18
(**10d**) $[Zn(C_{22}H_{32}N_4)(C_2H_3O_2)]PF_6 \cdot 0.5\ H_2O$	45.69	5.75	8.88	45.71	5.39	8.97

were precipitated from. Indeed, **10b** never did precipitate from methanol. Instead it was obtained by removing the methanol and stirring the residue in water to produce the pale blue powder product. Finally, the low yield of **9c** can be explained by the fact that two different colored solids precipitated from methanol, one red (**9c**) and another purple. Red **9c** was separated from the purple solid due to its lower solubility in methanol, whereas the purple solid could be dissolved away due to its higher methanol solubility. The purple solid is likely a configurational isomer of **9c**, due to its similar elemental analysis. Only **9c**, the higher-yielding product, was characterized for this study.

The purity of the complexes was examined by elemental analysis. "Pure" compounds generally have experimental percent C, H, and N values with 0.4% of their calculated values. Often, compounds absorb water from the air, which is called hygroscopy.

Six of the complexes are pure by this standard, although five of them appear hygroscopic, as additional amounts of water must be added to their formula to meet this standard. Two complexes, **10b** and **10c**, could not be made to fit a formula matching their experimental values sufficiently. Since both complexes are homogenous powders of typical colors for their metal ions and with acceptable mass spectrum peaks, it is anticipated that their true formulas will be discovered if and when an X-ray crystal structure is obtained in the future. All eight complexes gave crystals likely to yield structures when slow evaporation and ether-diffusion crystallization methods were applied. These crystals will be sent to a collaborator with the appropriate X-ray diffractometer for crystal structures to be obtained.

Comparison to cross-bridged complexes

Recall that the motivation of this work was to make complexes differing from the known cross-bridged analogues by only the lack of the cross-bridge itself. Ligands **11** and **12** in **Figure 6** have yielded complexes **13a-d** and **14a-d** in previous work in the Hubin labs. In this study, UV-Vis, magnetic moment, and cyclic voltammetry experiments will serve as points of comparison between the cross-bridged and unbridged complexes. These experiments examine the complexes' electronic properties, which if similar between bridged and unbridged analogues, would indicate that their d-electron configurations are also similar. Small differences in

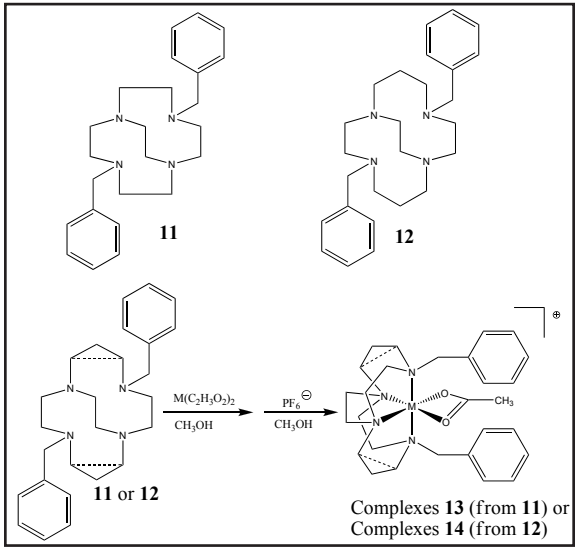

Figure 6. Cross-bridged ligands and complexes for comparison

d-electron configurations should result in only small differences in thermodynamic stabilities between the bridged and unbridged analogues. If future kinetic stability experiments show large (many orders of magnitude) differences in kinetic stability, the topological and rigidity constraints associated with the cross-bridge, rather than any inherent thermodynamic differences, are the likely (and hypothesized) cause of that kinetic stability.

UV-Visible spectroscopic values for the 12 UV-Visible active complexes **9a-c**, **10a-c**, **13a-c**, and **14a-c** are given in **Table 3** below. In all cases, **"a"** complexes are cobalt, **"b"** complexes are nickel, and **"c"** complexes are copper. Zinc **"d"** complexes are not UV-Visible active due to their d^{10} electron configurations, and are therefore not included. "λ_{max}" indicates peak locations (wavelength or color of absorbed light) and "ε" (extinction coefficient) indicates intensity of light absorption. All spectra were recorded in acetonitrile at similar concentrations.

In general, it is striking how similar the absorbance wavelengths and intensities are when comparing complexes that differ only due to the presence or absence of the cross-bridge. In most cases, wavelengths are within 10-30 nm and extinction coefficients are within 10-50 M-1 cm-1 of each other. **Figure 7** illustrates what a typical UV-Visible spectrum looks like and also shows, as an example, how similar spectra for Ni(**13b**) and Ni(**9b**) are. There are four absorbances at nearly the same wavelength and with nearly the same intensity for both complexes.

Two significantly different pairs are found in the copper complexes. In these cases, the cross-bridge is not the only difference in the structure. In cross-bridged Cu(**13c**) and Cu(**14c**), there is an additional acetate ligand (according to elemental analysis), while in the unbridged Cu(**9c**) and Cu(**10c**), the elemental analysis indicates there is no acetate ligand. In solution, the assumption is that the copper ions in Cu(**9c**) and Cu(**10c**) will become 5-coordinate by binding an acetonitrile solvent molecule, as indicated in the formulas in the **Table 3**. The identity of this fifth ligands, acetate vs. acetonitrile, clearly leads to large differences in the d-d absorption band. In the acetate-binding complexes, this band is between 708-

Table 3. Electronic spectra comparison

Complex	Metal ion	λ_{max} in nm (ε in M^{-1} cm^{-1}) [sh indicates a shoulder on another peak]			
Co(**13a**)$(C_2H_3O_2)^{2+}$	Co^{3+}	380 (235)	523 (356)		
Co(**9a**)$(C_2H_3O_2)^{+}$	Co^{2+}	372sh (50)	549 (58)		
Co(**14a**)$(C_2H_3O_2)^{+}$	Co^{2+}	464sh (17)	510 (20)	547sh (15)	
Co(**10a**)$(C_2H_3O_2)^{+}$	Co^{2+}	----	513 (32)	552sh (23)	
Ni(**13b**)$(C_2H_3O_2)^{+}$	Ni^{2+}	334 (37)	559 (10)	845sh (28)	951 (36)
Ni(**9b**)$(C_2H_3O_2)^{+}$	Ni^{2+}	364 (42)	587 (19)	820sh (21)	985 (48)
Ni(**14b**)$(C_2H_3O_2)^{+}$	Ni^{2+}	354 (15)	570 (7)	829sh (5)	979 (12)
Ni(**10b**)$(C_2H_3O_2)^{+}$	Ni^{2+}	364 (22)	579 (20)	814sh (20)	980 (18)
Cu(**13c**)$(C_2H_3O_2)^{+}$	Cu^{2+}	306 (6,490)	728 (140)		
Cu(**9c**)$(CH_3CN)^{2+}$	Cu^{2+}	301 (7,020)	607 (465)		
Cu(**14c**)$(C_2H_3O_2)^{+}$	Cu^{2+}	306 (6,930)	708 (150)		
Cu(**10c**)$(CH_3CN)^{2+}$	Cu^{2+}	282 (8,374)	528 (194)		

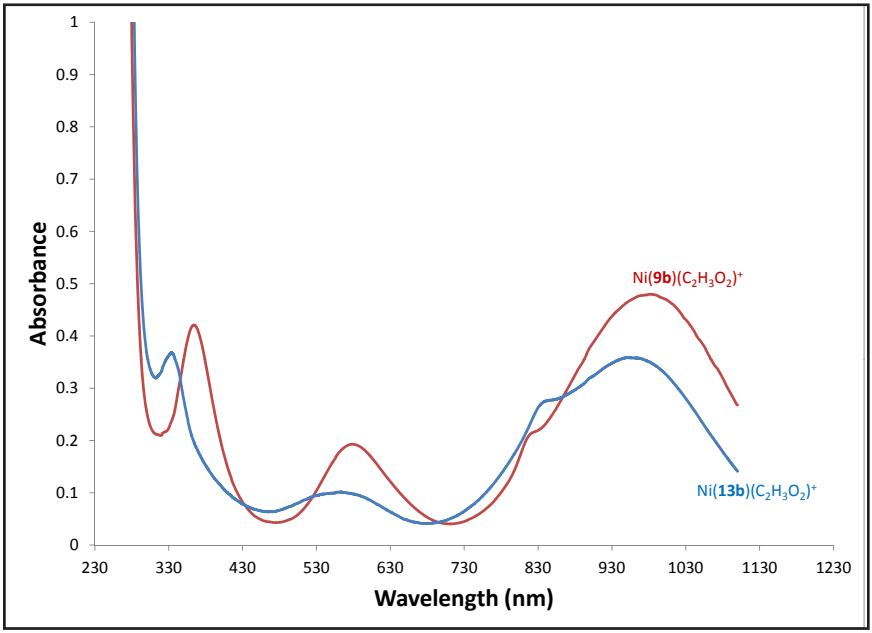

Figure 7. UV-Visible spectra of Ni(13) and Ni(9) in acetonitrile at 0.01 M

728 nm. However, the acetonitrile-binding complexes have the absorption between 528-607 nm. Acetate is negatively charged and binds copper through an oxygen donor. Acetonitrile is neutral and binds copper through a nitrogen donor. These differences would be expected to be evident in the UV-Visible spectrum, and indeed are, making these complexes less useful for determining the effect of the bridge only.

Another difference is seen in the Co(**13a**) vs Co(**9a**) pair. While the wavelengths are similar, the extinction coefficients are quite different. The Co(**13a**) complex was determined to have oxidized upon workup in air to the Co^{3+} cation, while the same workup of Co(**9a**) did not oxidize its Co^{2+} ion. Comparison with other cobalt complexes[2e,3a] of similar azamacrocycle ligands, the wavelengths and extinction coefficients are consistent with these observations. Again, this makes direct comparison of the effect of the bridge only impossible, since other factors have changed. The difference in ease of oxidation is likely present due to the distortion of the preferred octahedral geometry by the short cross-bridge. It forces the macrocyclic ligand to be folded tightly, and likely reduces the size of the cavity for metal binding. Oxidation to Co^{3+} results in a smaller metal ion than Co^{2+}, and is therefore apparently favored by the bridged ligand in Co(**13a**) over the more flexible unbridged ligand in the Co(**9a**) analogue. Interestingly, the Co(**14a**) and Co(**10a**) pair both remain in the Co^{2+} oxidation state. These ligands are both 14-membered rings, two carbons larger than the 12-membered **13a** and **9a** ligands. The larger rings appear to prefer larger Co^{2+} under the workup conditions.

Exploring the oxidation/reduction chemistry of these complexes, as discussed just above, can be done more directly through cyclic voltammetry experiments. In these experiments, the complexes in acetonitrile solution are subjected to a sweeping change in electrochemical potential, which can result in oxidation and reduction of the original metal ion. $E_{1/2}$ values (electrochemical potentials were oxidation/reduction occurs) and E_a-E_c values (reflecting how reversible the oxidation/reduction pair is) for these complexes are given in **Table 4**. $E_{1/2}$ values indicate coupled

oxidation/reduction pairs that are assigned to the complex which appears to undergo little change (such as gain/loss of ligands) other than the gain/loss of electrons. In these cases a small $E_{a-}E_c$ value indicates essentially no structural rearrangement upon oxidation/

Table 4. Redox potentials (vs. SHE) with peak separations.

Complex		**$E_{1/2}$ (V) Red Co^{3+}/Co^{2+}**	**(E_a-E_c) mV**	**$E_{1/2}$ (V) Red Co^{2+}/Co^{+}**	**(E_a-E_c) mV**
Co(**13a**)$(C_2H_3O_2)^{2+}$		+0.014	109	-0.640	178
Co(**9a**)$(C_2H_3O_2)^{+}$		+0.705 (ox only)	-----	+0.043 (red only)	-----
	E_{ox} (V) unassigned	**$E_{1/2}$ (V) #1**	**(E_a-E_c) mV**	**$E_{1/2}$ (V) #2**	**(E_a-E_c) mV**
Co(**14a**)$(C_2H_3O_2)^{+}$	+1.226	+0.638	75	+0.392	167
Co(**10a**)$(C_2H_3O_2)^{+}$	+0.754	+0.322	156	-0.301	266
	E_{ox} (V) Ni^{2+}/Ni^{3+}	**$E_{1/2}$ (V) Ni^{2+}/Ni^{3+}**	**(E_a-E_c) mV**	**E_{re} (V) Ni^{2+}/Ni^{+}**	
Ni(**13b**)$(C_2H_3O_2)^{+}$	+1.170	+1.117	106	-----	
Ni(**9b**)$(C_2H_3O_2)^{+}$	+1.230			-1.220	
Ni(**14b**)$(C_2H_3O_2)^{+}$	+1.255	-----	-----	-----	
Ni(**10b**)$(C_2H_3O_2)^{+}$	+1.290	-----	-----	-1.320	
Complex	**E_{ox} ($Cu^{2+/3+}$) [V]**	**E_{red} ($Cu^{2+/+}$) [V]**	**E_{ox} ($^{Cu+/2+}$) [V]**		
Cu(**13c**)$(C_2H_3O_2)^{+}$	+1.465	-0.637	-----		
Cu(**9c**)$(CH_3CN)^{2+}$	+1.280	-0.470	-0.240		
Cu(**14c**)$(OAc)^{+}$	+1.516	-0.641	-0.156		
Cu(**10c**)$(CH_3CN)^{2+}$	-----	-0.484	-0.208		

reduction, with 59 mV being the theoretical smallest value. Larger $E_{a-}E_c$ values indicate some structural changes that shift the partner event farther away than the theoretical value. E_{red} or E_{ox} are used when single oxidation or reduction processes are observed, but with no identifiable partner.

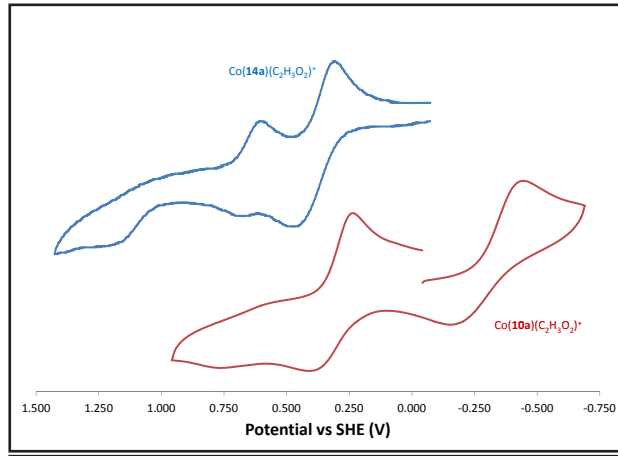

Figure 8. Cyclic Voltammograms of Co(14) and Co(10) in acetonitrile at 0.001 M

Although certain patterns of the numbers

and types of redox processes for each metal type are observed, many differences are seen between bridged and unbridged analogues. No bridged/unbridged pair gives nearly as similar behavior as in the UV-Visible spectra discussed above. **Figure 8** illustrates what a typical cyclic voltammogram looks like and also shows, as an example, how different voltammograms for Co(**14a**) and Co(**10a**) are. Co(**14a**) has only oxidations, with two reversible processes around +0.500 V, and an additional irreversible process near +1.200 V. Co(**10a**), while giving the same number of peaks, has one quasi-reversible reduction in the negative region (near -0.300 V) and only one reversible oxidation. Although the curves look similar in shape, the potential shifts are large and the types of processes each complex undergoes are significantly different.

While it is possible to discuss each bridged/unbridged pair in turn, we will not do so because such a discussion would be long, tedious, and difficult to follow since there are rather large changes in many cases, which don't necessarily correlate between different bridged/unbridged pairs. Instead, we will speculate on why the electrochemical behavior is so different when the bridge is removed, while the UV-Visible spectra change so little. A primary reason is likely the static nature of the UV-Visible spectrum versus the dynamic reactivity inherent to cyclic voltammetry. The UV-Visible spectrum is obtained on a complex without causing it to change in any way, thus you get information on the unreacted complex as it exists in a single structure in solution. According to the highly congruent UV-Visible data, our initial bridged and unbridged complexes are structurally very similar to one another, with the presence or absence of the bridge making little difference except in the preference for Co^{2+}/Co^{3+} in the Co(**13a**)/Co(**9a**) case and the preference for acetate anion binding the bridged/unbridged copper complexes discussed above.

However, the cyclic voltammetry experiment is a dynamic one, where complexes gain and lose d-electrons in response to the electrical potential they are subjected to. Once oxidation or reduction takes place, complexes may structurally rearrange in response to the new d-electron configuration, or even gain or lose

ligands due to the preference of the new metal ion oxidation state. Perhaps it should not be surprising that the presence/absence of the 2-carbon cross-bridge leads to quite different structural rearrangements and/or ligand gains/losses, as demonstrated by the significant differences in electrochemical behavior between complexes differing only by the bridge. Additional studies will continue to probe these differences. Particularly, kinetic stability experiments are needed to determine the effects of the bridge. From the data presented, it is clear that the kinetic experiments will need to be carried out under conditions where the electrochemical potential is static, so the complexes are electronically as similar as possible, as in the UV-Visible experiments above.

Acknowledgements

We thank the Chemistry Department of Southwestern Oklahoma State University for its support of this work, which was carried in the Fall 2013 Inorganic Chemistry Lab course CHEM 3211. TJH acknowledges the Oklahoma Center for the Advancement of Science and Technology for support through Grant Number HR13-157-1. Acknowledgement is made to the Donors of the American Chemical Society Petroleum Research Fund for partial support of this research.

References

1. Busch, D. H. Chem. Rev. 1993, 93, 847.
2. a) Hubin, T. J.; McCormick, J. M.; Collinson, S. R.; Alcock, N. W.; Busch, D. H. *J. Chem. Soc., Chem. Commun.*, **1998**, 1675-1676. b) Hubin, T. J.; McCormick, J. M.; Alcock, N. W.; Clase, H. J.; Busch, D. H. *Inorg. Chem.*, **1999**, *38*, 4435. c) Hubin, T. J.; McCormick, J. M.; Collinson, S. R.; Perkins, C. M.; Alcock, N. W.; Kahol, P. K.; Raghunathan, A.; Busch, D. H. *J. Am. Chem. Soc.*, **2000**, *122*, 2512. d) Hubin, T. J. *Coord. Chem. Rev.*, **2003**, *241*, 27. e) Hubin, T. J.; Alcock, N. W.; Clase, H. J.; Seib, L.; Busch, D. H. *Inorg. Chim. Acta*, **2002**, *337*, 91.
3. a) Hung, Y.; Martin, L. Y.; Jackels, S. C.; Tait, A. M.; Busch, D. H. *J. Am. Chem. Soc.*, **1977**, *99*, 4029. b) Martin, L. Y.; Sperati, C. R.; Busch, D. H. *J. Am. Chem. Soc.*, **1977**, *99*, 2968.
4 a) Royal, G.; Dahaoui-Gindrey, V.; Dahaoui, S.; Tabard, A.; Guilard, R.; Pullumbi, P.; Lecomte, *C. Eur. J. Org. Chem.*, **1998**, 1971-1975. b) Springborg, J.; Kofod, P.; Olsen, C. E.; Toftlund, H.; Sotofte, I. *Acta Chem. Scand.*, **1995**, *49*, 547-554. c) Yoo, J. S.; Darpan, P. WO 2011/031073 A2.

5. a) DeRosa, F.; Xianhu, B.; Ford, P. C. *Inorg. Chem.* **2003**, *42*, 4171-4178. b) Gasnier, A.; Royal, G.; Terech, P. *Langmuir*, **2009**, *25*, 8751-8762. c) Dong, Y.; Farquhar; S.; Gloe, K.; Lindoy, L. F.; Rumbel, B. R.; Turner, P.; Wichmann, K. *Dalton Trans*. **2003**, *8*, 1558-1566. d) Dong, Y.; Lawrence, G. A.; Lindoy, L. F.; Turner, P. *Dalton Trans*. **2003**, 1567-1576. e) Dong, Y.; Lindoy, L. F.; Turner, P. *Aust. J. Chem*. **2005**, *58*, 339-344.
6. Perrin, D. D.; Armarego, W. L. F.; Perrin, D. R. Purification of Laboratory Chemicals, 2nd Ed., Pergamon Press: New York, 1980.
7. Barefield, E. K.; Wagner, F.; Herlinger, A. W.; Dahl, A. R. *Inorg. Synth.,* **1976**, *16*, 220.

Ashlie Walker

Megan Ayala

Mackenzie Bergagnini

Stephanie Chidester

Chad Doeden

John Bui

Louis Esjornson

Brian R. Sweany

Dr. Tim Hubin